Polarimetric Formulation of the Visibility Function Equation Including Cross-Polar Antenna Patterns

Adriano Camps, *Senior Member, IEEE*, Ignasi Corbella, *Member, IEEE*, Francesc Torres, *Member, IEEE*, Mercè Vall-llossera, *Member, IEEE*, and Nuria Duffo, *Member, IEEE*

***Abstract*—The European Space Agency's Soil Moisture and Ocean Salinity (SMOS) mission will be the first one using two-dimensional aperture synthesis radiometry for earth observation. This study presents the formulation that relates instrument observables and brightness temperature maps including cross-polar antenna voltage patterns, which may be also different from element to element. Finally, the radiometric accuracy degradation if cross-polar patterns are neglected in the image reconstruction is studied.**

***Index Terms*—Antenna arrays, interferometry, radiometry.**

I. Introduction

THE Microwave Imaging Radiometer by Aperture Synthesis (MIRAS) instrument [1], [2] is the single payload of the European Space Agency's Soil Moisture and Ocean Salinity (SMOS) mission, and it will be the first two-dimensional aperture synthesis radiometer for earth observation. The brightness temperature image reconstruction is performed through a Fourier synthesis process of the cross-correlations V_{12}^{pq} measured between the band pass signals $b_1(t)$ and $b_2(t)$ -centered at f_0, $\lambda_0 = c/f_0$- collected by every pair of elements in the array located in the XY plane. According to [3]

$$\begin{aligned} V_{12}^{pq} &\triangleq \frac{1}{k_B\sqrt{B_1B_2}\sqrt{G_1G_2}} \cdot \frac{1}{2}\left\langle b_1^p(t) b_2^{q^*}(t)\right\rangle \\ &= \frac{1}{\sqrt{\Omega_1\Omega_2}} \int\int_{\xi^2+\eta^2\le 1} \frac{(T_{pq}(\xi,\eta) - T_{\rm rec}\delta_{pq})}{\sqrt{1-\xi^2-\eta^2}} \\ &\quad \cdot F_{np1}(\xi,\eta) F_{nq2}^*(\xi,\eta)\, \tilde{r}_{12}\left(-\frac{u_{12}\xi + v_{12}\eta}{f_0}\right) \\ &\quad \cdot \exp\left(-j2\pi(u_{12}\xi + v_{12}\eta)\right) d\xi d\eta \end{aligned} \tag{1}$$

where k_B is the Boltzmann's constant, $B_{1,2}$ and $G_{1,2}$ are the receivers' noise bandwidth and power gain, $\Omega_{1,2}$ is the solid angle of the antennas, $T_{pq}(\xi,\eta)$ is the brightness temperature of the scene [see (4)], $T_{\rm rec}$ is the physical temperature of the receivers [3], $\delta_{pq} = 1$ if $p = q$ and 0 if $p \neq q$, $F_{np,q1,2}(\xi,\eta)$ are the normalized antenna copolar voltage patterns at p and q polarizations, $\tilde{r}_{12}(-(u_{12}\xi + v_{12}\eta)/f_0)$ is the fringe-washing function, (u_{12}, v_{12}) is the spatial frequency (baseline) that depends on the antenna position difference: $(u_{12}, v_{12}) = (x_2 - x_1, y_2 - y_1)/\lambda_0$, and the director cosines $(\xi,\eta) = (\sin\theta\cos\phi, \sin\theta\sin\phi)$ are defined with respect to the X and Y axes.

Manuscript received October 10, 2003; revised February 4, 2004. This work was supported in part by the Spanish Comisión Interministerial de Ciencia y Tecnología under Grant MCYT TIC2002-04451-C02-01 and in part by EADS-CASA Space Division (Madrid, Spain), prime contractor of SMOS PLM during Phase B Activities.

The authors are with the Universitat Politècnica de Catalunya, E-08034 Barcelona, Spain (e-mail: camps@tsc.upc.es).

Digital Object Identifier 10.1109/LGRS.2005.846885

II. Brightness Temperature Measured by the Interferometric Radiometer: Ideal Case With Isotropic Antenna Voltage Patterns and Zero Cross-Polar Patterns

Due to the following:

- the relative orientation $[\psi(\xi,\eta)]$ between the pixel's reference frame over the earth's surface (V or H: vertical and horizontal polarizations) and the antenna reference frame [4] (X is perpendicular to the orbital plane; Y is 32° upward titled from the velocity vector);
- Faraday rotation effects $[\phi(\xi,\eta)]$

the electric fields incident in the antennas are rotated an angle $\alpha(\xi,\eta) = \psi(\xi,\eta) + \phi(\xi,\eta)$ [4]

$$\begin{bmatrix} E_x \\ E_y \end{bmatrix} = \begin{bmatrix} A & B \\ -B & A \end{bmatrix} \begin{bmatrix} E_h \\ E_v \end{bmatrix} \tag{2}$$

where $A = \cos(\alpha)$, $B = \sin(\alpha)$. Therefore, since $T_{pq}(\xi,\eta)$ is proportional to $\langle E_p E_q^*\rangle/2$, the brightness temperatures in the antenna reference frame at a given polarization (X or Y) can be expressed as a linear combination of the brightness temperatures in the earth's pixel reference frame (H or V) [5, eq. (57)].

$$\begin{bmatrix} T_{xx} \\ T_{xy} \\ T_{yx} \\ T_{yy} \end{bmatrix} = \begin{bmatrix} A^2 & AB & AB & B^2 \\ -AB & A^2 & -B^2 & AB \\ -AB & -B^2 & A^2 & AB \\ B^2 & -AB & -AB & A^2 \end{bmatrix} \begin{bmatrix} T_{hh} \\ T_{hv} \\ T_{vh} \\ T_{vv} \end{bmatrix} \tag{3}$$

where $T_{vh} = T_{hv}^* \hat{=} (U + jV)/2$, and U and V are the third and fourth Stokes parameters in the earth's reference frame. Compared to T_{hh} and T_{vv}, U and V have negligible values, and even more at L-band. Therefore, $\mathrm{Im}(T_{xy}) = \mathrm{Im}(T_{yx}) = 0$ and $\mathrm{Re}(T_{xy}) = \mathrm{Re}(T_{yx})$, and $T_{xy} = T_{yx} = \mathrm{Re}(T_{xy}) = \mathrm{Re}(T_{yx})$. Equation (3) reduces to

$$\begin{bmatrix} T_{xx} \\ T_{yx} \\ T_{yy} \end{bmatrix} = \begin{bmatrix} A^2 & B^2 \\ -AB & AB \\ B^2 & A^2 \end{bmatrix} \begin{bmatrix} T_{hh} \\ T_{vv} \end{bmatrix}. \tag{4}$$

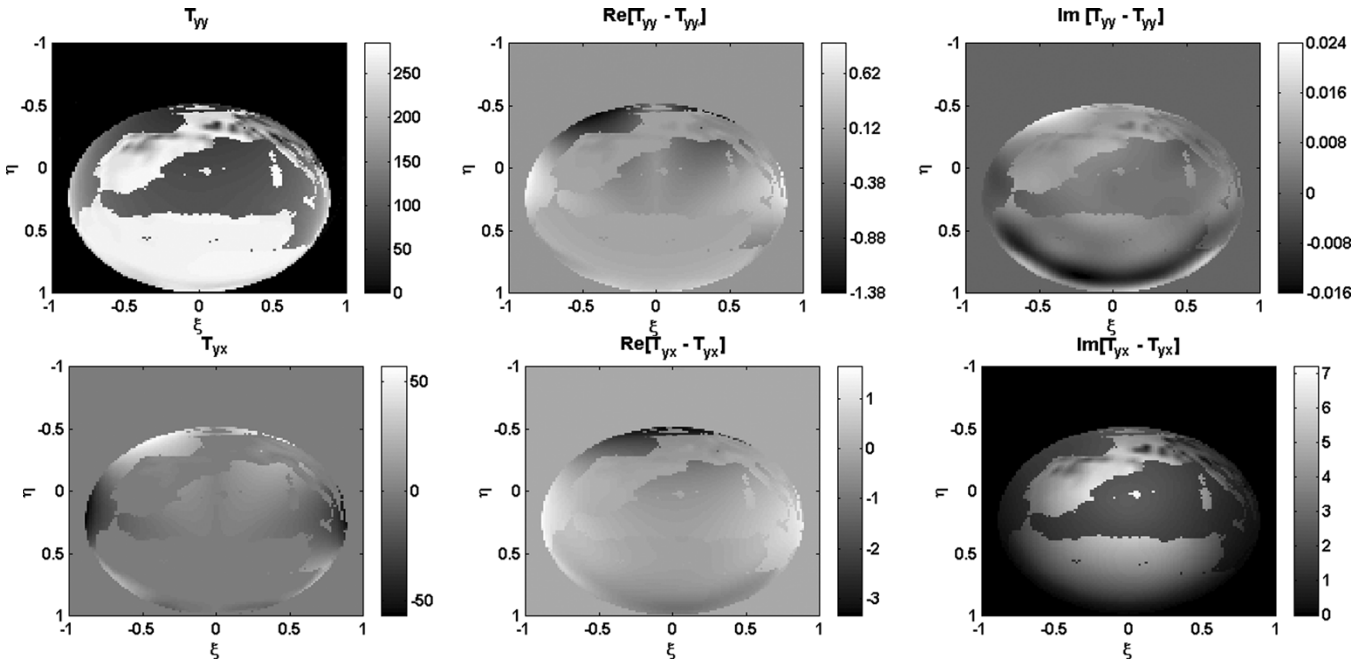

Fig. 1. Image errors maps in a high-contrast scene if antenna cross-polarization patterns are neglected: $T_{yy} = A^2 T_{vv} + B^2 T_{hh}$ and $T_{yx} = AB\,(T_{vv} - T_{hh})$. Root mean squared errors in the alias-free field of view: $\sigma_{\mathrm{Re}[\hat{T}_{xx} - \hat{T}^{id}_{xx}]} = 0.18$ K, $\sigma_{\mathrm{Im}[\hat{T}_{xx} - \hat{T}^{id}_{xx}]} = 5.5\ 10^{-3}$ K, $\sigma_{\mathrm{Re}[\hat{T}_{yy} - \hat{T}^{id}_{yy}]} = 0.15$ K, $\sigma_{\mathrm{Im}[\hat{T}_{yy} - \hat{T}^{id}_{yy}]} = 3.6\ 10^{-3}$ K, $\sigma_{\mathrm{Re}[\hat{T}_{yx} - \hat{T}^{id}_{yx}]} = 0.30$ K and $\sigma_{\mathrm{Im}[\hat{T}_{yx} - \hat{T}^{id}_{yx}]} = 3.5$ K.

III. Brightness Temperature Measured by the Interferometric Radiometer: Real Case Including Antenna Copolar and Nonzero Cross-Polar Patterns

If nonzero cross-polar antenna patterns are taken into account, a similar process to the one followed to derive (2)–(4), can be used to derive the cross-brightness temperatures to be used in (1)

$$\begin{bmatrix} \hat{E}_{x1,2} \\ \hat{E}_{y1,2} \end{bmatrix} = \begin{bmatrix} R_{x1,2} & C_{x1,2} \\ C_{y1,2} & R_{y1,2} \end{bmatrix} \begin{bmatrix} E_{x1,2} \\ E_{y1,2} \end{bmatrix} \tag{5}$$

where the symbol $\hat{E}_{x,y1,2}$ denotes the received electric field including the effect of the antenna voltage patterns, $R_{x,y1,2}(\xi,\eta) \equiv F_{nx,y1,2}(\xi,\eta)$ is the copolar pattern of antenna 1 or 2, at X or Y polarization, and $C_{x,y1,2}(\xi,\eta)$ is the cross-polar antenna pattern, both normalized to the maximum of $R_{x,y1,2}(\xi,\eta)$, and defined according to Ludwig's third definition [6].[1] Expanding (5), the relationship between $\hat{T}_{xx}, \hat{T}_{yy}$ and $\hat{T}_{yx}$ and T_{xx}, T_{yy} and T_{xy} can be readily obtained

$$\hat{T}_{xx} = R_{x1}R^*_{x2}T_{xx} + (R_{x1}C^*_{x2} + C_{x1}R^*_{x2})\,T_{yx} + C_{x1}C^*_{x2}T_{yy} \tag{6}$$

$$\hat{T}_{yy} = C_{y1}C^*_{y2}T_{xx} + \left(R_{y1}C^*_{y2} + C_{y1}R^*_{y2}\right)T_{yx} + R_{y1}R^*_{y2}T_{yy} \tag{7}$$

$$\hat{T}_{yx} = C_{y1}R^*_{x2}T_{xx} + (R_{y1}R^*_{x2} + C_{y1}C^*_{x2})\,T_{yx} + R_{y1}C^*_{x2}T_{yy}. \tag{8}$$

The term "T_{rec}" in (1) accounts for the thermal noise radiated by the receivers at both polarizations (but not at the cross-polar one) that is collected by other elements because of the nonzero antenna coupling. This noise is collected together with the noise coming from the scene being imaged. Therefore, following a similar procedure to the one described in previous paragraphs for T_{pq}, (1) should be modified for the T_{rec} term accordingly

$$\begin{aligned} \hat{T}_{\mathrm{rec}\,xx} &= R_{x1}R^*_{x2}T_{\mathrm{rec}} + C_{x1}C^*_{x2}T_{\mathrm{rec}} \\ \hat{T}_{\mathrm{rec}\,yy} &= C_{y1}R^*_{x2}T_{\mathrm{rec}} + R_{y1}C^*_{x2}T_{\mathrm{rec}} \\ \hat{T}_{\mathrm{rec}\,yx} &= 0. \end{aligned} \tag{9}$$

Substituting (6)–(9) in (1), (1) can be rewritten making the following substitutions, as in (10), shown at the bottom of the page, where it has been assumed that $T_{yx} = T_{xy}$.

[1] In (5) the measured co- and cross-polar patterns at X- and Y -polarizations correspond to the two outputs of a dual-polarization antenna as normally measured. If the Y -pattern were obtained by a rotation of the X -pattern, then the cross-polar pattern $C_{y1,2}$ must be replaced by $-C_{y1,2}$.

$$\begin{aligned} (T_{xx}(\xi,\eta) - T_{\mathrm{rec}})\,F_{n\,x1}(\xi,\eta)\,F^*_{n\,x2}(\xi,\eta) &\rightarrow R_{x1}R^*_{x2}(T_{xx} - T_{\mathrm{rec}}) + (R_{x1}C^*_{x2} + C_{x1}R^*_{x2})\,T_{yx} + C_{x1}C^*_{x2}(T_{yy} - T_{\mathrm{rec}}), \\ (T_{yy}(\xi,\eta) - T_{\mathrm{rec}})\,F_{n\,y1}(\xi,\eta)\,F^*_{n\,y2}(\xi,\eta) &\rightarrow C_{y1}C^*_{y2}(T_{xx} - T_{\mathrm{rec}}) + \left(R_{y1}C^*_{y2} + C_{y1}R^*_{y2}\right)T_{yx} + R_{y1}R^*_{y2}(T_{yy} - T_{\mathrm{rec}}), \\ T_{yx}(\xi,\eta)\;F_{n\,y1}(\xi,\eta)\,F^*_{n\,x2}(\xi,\eta) &\rightarrow C_{y1}R^*_{x2}(T_{xx} - T_{\mathrm{rec}}) + (R_{y1}R^*_{x2} + C_{y1}C^*_{x2})\,T_{yx} + R_{y1}C^*_{x2}(T_{yy} - T_{\mathrm{rec}}) \end{aligned} \tag{10}$$

IV. Errors Associated to Nonzero Cross-Polar Antenna Patterns in the Image Reconstruction Algorithms in the Antenna Reference Frame

In order to study the impact of neglecting antenna cross-polar pattern in the image reconstruction algorithms, synthetic brightness temperature images have been generated using the SMOS End-to-end Performance Simulator (SEPS) [7]. The co- and cross-polar antenna radiation voltage patterns used correspond to the first nine receiver units (LICEF-2) of MIRAS and exhibit a directivity of 9 dB approximately, with cross-polar level at boresight of -30 dB approximately, and -25 dB worst case at the border of the alias-free field of view, which is determined by the periodic repetition of six replicas of the earth's image [7].

Fig. 1 (top) shows the difference between T_{yy} when the cross-polar component of the antenna voltage patterns is assumed to be zero, and (7) with nonzero cross-polar component, for a high-contrast scenario, including land and sea. Fig. 1 (bottom) presents a similar result for T_{yx}. Error images at X polarization are very similar to the ones at Y polarization, and are not shown. The rms errors computed in the alias-free field-of-view at different polarizations are: $\sigma_{\mathrm{Re}[\hat{T}_{xx}-\hat{T}^{id}_{xx}]} = 0.18$ K, $\sigma_{\mathrm{Im}[\hat{T}_{xx}-\hat{T}^{id}_{xx}]} = 5.5\ 10^{-3}$ K, $\sigma_{\mathrm{Re}[\hat{T}_{yy}-\hat{T}^{id}_{yy}]} = 0.15$ K, $\sigma_{\mathrm{Im}[\hat{T}_{yy}-\hat{T}^{id}_{yy}]} = 3.6\ 10^{-3}$ K, $\sigma_{\mathrm{Re}[\hat{T}_{yx}-\hat{T}^{id}_{yx}]} = 0.30$ K and $\sigma_{\mathrm{Im}[\hat{T}_{yx}-\hat{T}^{id}_{yx}]} = 3.5$ K where the superscript "*id*" refers to the $\hat{T}_{pq}$ if the cross-polar patterns were zero. It would be expected that the smaller the difference between T_{yy} and T_{xx}, the smaller the effect of nonzero cross-polar pattern errors. However, a low-contrast only-ocean scene has similar errors at X- and Y- polarizations, and just slightly smaller at YX-polarization: $\sigma_{\mathrm{Re}[\hat{T}_{yx}-\hat{T}^{id}_{yx}]} = 0.48$ K, and $\sigma_{\mathrm{Im}[\hat{T}_{yx}-\hat{T}^{id}_{yx}]} = 1.9$ K. Errors in the imaginary parts of T_{xx} and T_{yy} come from neglecting cross-polar antenna patterns in the image reconstruction. At the present time there is not an explanation for the fact that the error on T_{yx} is found with the same sign throughout the field of view, but it is believed that it may be due to a phase offset between the Y and X antenna patterns, due to different path lengths from the antenna to the receivers' input.

V. Error Amplification in the Transformation From Antenna Reference Frame to Earth Reference Frame

MIRAS has two operation modes.

- Full-polarimetric mode, in which $\hat{T}_{xx}$, $\hat{T}_{yy}$ and $\hat{T}_{xy}$ are measured by a sophisticated combination of the antenna polarization switches at X and Y polarizations [5], and
- Dual-polarization mode, in which $\hat{T}_{xx}$ and $\hat{T}_{yy}$ are sequentially measured, by selecting all the antenna polarization switches at X and Y polarizations simultaneously.

In the full-polarimetric mode, the brightness temperatures in the earth reference frame ($\hat{T}_{hh}$, $\hat{T}_{vv}$, $\hat{T}_{hv}$, and $\hat{T}_{vh}$) are computed from the measured brightness temperatures in the antenna reference frame ($\hat{T}_{xx}$, $\hat{T}_{yy}$, $\hat{T}_{xy}$ and $\hat{T}_{yx}$) by inverting (3)

$$\begin{bmatrix} \hat{T}_{hh} \\ \hat{T}_{hv} \\ \hat{T}_{vh} \\ \hat{T}_{vv} \end{bmatrix} = \begin{bmatrix} A^2 & -AB & -AB & B^2 \\ AB & A^2 & -B^2 & -AB \\ AB & -B^2 & A^2 & -AB \\ B^2 & AB & AB & A^2 \end{bmatrix} \begin{bmatrix} \hat{T}_{xx} \\ \hat{T}_{xy} \\ \hat{T}_{yx} \\ \hat{T}_{yy} \end{bmatrix} \quad (11)$$

and errors in the antenna reference frame translate into errors in the earth reference frame

$$\begin{bmatrix} \Delta\hat{T}_{hh} \\ \Delta\hat{T}_{hv} \\ \Delta\hat{T}_{vh} \\ \Delta\hat{T}_{vv} \end{bmatrix} = \begin{bmatrix} A^2 & -AB & -AB & B^2 \\ AB & A^2 & -B^2 & -AB \\ AB & -B^2 & A^2 & -AB \\ B^2 & AB & AB & A^2 \end{bmatrix} \begin{bmatrix} \Delta\hat{T}_{xx} \\ \Delta\hat{T}_{xy} \\ \Delta\hat{T}_{yx} \\ \Delta\hat{T}_{yy} \end{bmatrix}. \quad (12)$$

Note that the inverse of the matrix in (3) is equal to its transpose.

In the dual-polarization mode, the brightness temperatures in the earth reference frame ($\hat{T}_{hh}$ and $\hat{T}_{vv}$) are computed from (4), assuming $T_{yx} = 0$

$$\begin{bmatrix} \hat{T}_{hh} \\ \hat{T}_{vv} \end{bmatrix} = \frac{1}{A^4 - B^4} \begin{bmatrix} A^2 & -B^2 \\ -B^2 & A^2 \end{bmatrix} \begin{bmatrix} \hat{T}_{xx} \\ \hat{T}_{yy} \end{bmatrix} \quad (13)$$

and errors in the antenna reference frame translate into errors in the earth reference frame

$$\begin{bmatrix} \Delta\hat{T}_{hh} \\ \Delta\hat{T}_{vv} \end{bmatrix} = \frac{1}{A^4 - B^4} \begin{bmatrix} A^2 & -B^2 \\ -B^2 & A^2 \end{bmatrix} \begin{bmatrix} \Delta\hat{T}_{xx} \\ \Delta\hat{T}_{yy} \end{bmatrix}. \quad (14)$$

Note that the errors tend to infinite wherever $A = B$, as studied in [8].

Errors in $\mathrm{Im}[\hat{T}_{yx} - \hat{T}^{id}_{yx}]$ [see (8)] are specially important because of the phase difference between the co- and cross-polar antenna voltage patterns, and may ultimately limit the capabilities of using the measurement of the third Stokes parameter to correct for Faraday rotation effects[2] [see (8)] [9], necessary to derive T_{hh} and T_{vv} accurately.[3] Additionally, even though the measurement of $\hat{T}_{yx}$ allows to obtain $\hat{T}_{hh}$ and $\hat{T}_{vv}$ maps in the whole alias-free field of view without singularities [see (11); matrix in (3) is never singular], errors in $\hat{T}_{yx}$ directly translate into $\hat{T}_{hh}$ and $\hat{T}_{vv}$ through (12). The singularity problem can be avoided and cross-polar pattern errors minimized if the geophysical parameter retrieval algorithms are designed to operate with brightness temperature maps in the antenna reference frame—although Faraday rotation correction will still be necessary—or to operate on $\hat{I} = \hat{T}_{xx} + \hat{T}_{yy} = \hat{T}_{hh} + \hat{T}_{vv}$, which is invariant to rotations (see [11] for ocean salinity retrieval study). $\hat{I}$ can be computed as $\hat{I} = \hat{T}_{xx} + \hat{T}_{yy}$, where $\hat{T}_{xx}$ and $\hat{T}_{yy}$ are measured in the dual polarization mode.

VI. Conclusion

This work has presented the extension of the formulation of the visibility function to include the cross-polar voltage patterns, which may be different from element to element. Its impact on the radiometric accuracy has been analyzed using SEPS and antenna patterns measured by EADS-CASA espacio for the first nine MIRAS receivers, showing a degradation smaller than 0.18 K root mean square within the alias-free field of view.

[2]The average daytime Faraday rotation at L-band is $17^\circ/f^2$ (f in gigahertz), which is 8.7° approximately [10]. However, it can exhibit very large variations, depending on the local time, season, solar activity, and geographic location.

[3]The brightness temperature sensitivity to sea surface salinity is 0.5 K/psu at 25 °C, and the salinity retrieval accuracy is 0.1 psu after spatio-temporal averaging in 200-km boxes and 30 days.

REFERENCES

[1] M. Martín-Neira and J. M. Goutoule, "MIRAS—A two-dimensional aperture-synthesis radiometer for soil-moisture and ocean salinity observations," *ESA Bull.*, no. 92, pp. 95–104, Nov. 1997.

[2] P. Sivestrin, M. Berger, Y. Kerr, and J. Font, "ESA's second earth explorer opportunity mission: The Soil Moisture and Ocean Salinity mission—SMOS," *IEEE Geosci. Remote Sens. Newslett.*, no. 118, pp. 11–14, 3 2001.

[3] I. Corbella, N. Duffo, M. Vall-llossera, A. Camps, and F. Torres, "The visibility function in interferometric aperture synthesis radiometry," *IEEE Trans. Geosci. Remote Sens.*, vol. 42, no. 8, pp. 1677–1682, Aug. 2004.

[4] J. P. Claassen and A. K. Fung, "The recovery of polarized apparent temperature distributions of flat scenes from antenna temperature measurements," *IEEE Trans. Antennas Propagat.*, vol. AP-22, pp. 433–442, 1974.

[5] M. Martín-Neira, S. Ribó, and A. J. Martín-Polegre, "Polarimetric mode of MIRAS," *IEEE Trans. Geosci. Remote Sens.*, vol. 40, no. 8, pp. 1755–1768, Aug. 2002.

[6] A. C. Ludwig, "The definition of cross polarization," *IEEE Trans. Antennas Propagat.*, vol. AP-21, no. 1, pp. 116–119, Jan. 1973.

[7] A. Camps, I. Corbella, M. Vall-llossera, N. Duffo, F. Marcos, F. Martínez-Fadrique, and M. Greiner, "The SMOS end-to-end performance simulator: Description and scientific applications," in *Proc. IGARSS*, vol. 1, Toulouse, France, Jul. 21–25, 2003, pp. 13–15.

[8] P. Waldteufel and G. Caudal, "About off-axis radiometric polarimetric measurements," *IEEE Trans. Geosci. Remote Sens.*, vol. 40, no. 6, pp. 1435–1439, Jun. 2002.

[9] S. H. Yueh, "Estimates of faraday rotation with passive microwave polarimetry for microwave remote sensing of earth surfaces," *IEEE Trans. Geosci. Remote Sens.*, vol. 38, no. 9, pp. 2434–2438, Sep. 2000.

[10] J. P. Hollinger and R. C. Lo, "Low-frequency microwave radiometer for N-ROSS, in Large Space Antenna Sys. Technol.," in *NASA Conf. Publ.*, vol. 2368, 1984, pp. 87–95.

[11] A. Camps, I. Corbella, M. Vall-llossera, N. Duffo, F. Torres, R. Villarino, L. Enrique, F. Julbé, J. Font, A. Julià, C. Gabarró, J. Etchetto, J. Boutin, A. Weill, V. Caselles, E. Rubio, P. Wursteisen, and M. Martín-Neira, "L-Band sea surface emissivity: Preliminary results of the WISE-2000 campaign and its application to salinity retrieval in the SMOS mission," *Radio Sci.*, vol. 38, no. 4, pp. 8071–8071, Jun. 2003. DOI: 10.1029/2002RS002629.